Vol. 542: 51–62, 2016
doi: 10.3354/meps11539

MARINE ECOLOGY PROGRESS SERIES
Mar Ecol Prog Ser

Published January 19

FREE ACCESS

Photoacclimation of natural phytoplankton communities

Jason R. Graff[1,*], Toby K. Westberry[1], Allen J. Milligan[1], Matthew B. Brown[1], Giorgio Dall'Olmo[2], Kristen M. Reifel[1], Michael J. Behrenfeld[1]

[1]Oregon State University, Department of Botany and Plant Pathology, 2082 Cordley Hall, Corvallis, OR 97330, USA
[2]Plymouth Marine Laboratory, United Kingdom and National Centre for Earth Observation, Prospect Place, The Hoe, Plymouth, UK

ABSTRACT: Phytoplankton regulate internal pigment concentrations in response to light and nutrient availability. Chlorophyll *a* to phytoplankton carbon ratios (chl:C_{phyto}) are commonly reported as a function of growth irradiance (E_g) for evaluating the photoacclimation response of phytoplankton. In contrast to most culture experiments, natural phytoplankton communities experience fluctuating environmental conditions, making it difficult to compare field and lab observations. Observing and understanding photoacclimation in nature is important for deciphering changes in chl:C_{phyto} resulting from environmental forcings and for accurately estimating net primary production (NPP) in models which rely on a parameterized description of photoacclimation. Here we employ direct analytical measurements of C_{phyto} and parallel high-resolution biomass estimates from particulate backscattering (b_{bp}) and flow cytometry to investigate chl:C_{phyto} in natural phytoplankton communities. Chl:C_{phyto} observed over a wide range of E_g in the field was consistent with photoacclimation responses inferred from satellite observations. Field-based photoacclimation observations for a mixed natural community contrast with laboratory results for single species grown in continuous light and nutrient-replete conditions. Applying a carbon-based NPP model to our field data for a north–south transect in the Atlantic Ocean results in estimates that closely match ^{14}C depth-integrated NPP for the same cruise and with historical records for the distinct biogeographic regions of the Atlantic Ocean. Our results are consistent with previous satellite and model observations of cells growing in natural or fluctuating light and showcase how direct measurements of C_{phyto} can be applied to explore phytoplankton photophysiology, growth rates, and production at high spatial resolution *in situ*.

KEY WORDS: Phytoplankton carbon · Chlorophyll · Growth irradiance · Photoacclimation · Growth rate · Primary production · Nutrients

INTRODUCTION

Photoacclimation is the phenotypic response of cells to changes in their light environment (Falkowski & LaRoche 1991, MacIntyre et al. 2002). This response includes changes in enzymatic processes, morphology, and biochemical composition. One of the most extensively documented forms of photoacclimation is the change in cellular pigment concentration as a function of growth irradiance, a response that can be quantified by changes in chlorophyll *a*: phytoplankton carbon (chl:C_{phyto}) ratios. Chl:C_{phyto} variability, however, is not simply a function of growth irradiance but also registers changes in nutrient-driven division rate and other environmental conditions.

Phytoplankton cultures grown under nutrient replete conditions in the laboratory exhibit maximum

*Corresponding author: jrgraff@science.oregonstate.edu

chl:C_{phyto} values and minimum growth rate (μ) at low growth irradiances (E_g) and minimum chl:C_{phyto} and maximum μ at high E_g (e.g. Fig. 1, dashed line) (Cloern et al. 1995, Geider et al. 1997, Halsey & Jones 2015). In contrast, nutrient-limited phytoplankton grown under constant E_g exhibit maximum chl:C_{phyto} at high μ and minimum chl:C_{phyto} at low μ (Laws & Bannister 1980, Halsey et al. 2013). Such laboratory results emphasize that chl:C_{phyto} is dependent on light and nutrient status, both of which must always be considered when evaluating phytoplankton photophysiology in natural phytoplankton populations.

In situ light fields fluctuate on timescales ranging from seconds in near surface waters (Schubert et al. 2001) to vertical mixing dynamics that range from hours to days (Denman & Gargett 1983, Backhaus et al. 1999, D'Asaro 2008) to seasonal patterns in incident light. Phytoplankton respond to fluctuating light by altering their cellular chl and carbon content on time scales less than 1 h (Lewis et al. 1984, Cullen & Lewis 1988, Havelková-Doušová et al. 2004) and employ photoprotective mechanisms such as non-photochemical quenching (Havelková-Doušová et al. 2004, Miloslavina et al. 2009, van de Poll et al. 2010, Milligan et al. 2012, Alderkamp et al. 2013) that are active on timescales of microseconds to minutes.

Phytoplankton growth conditions in the field contrast starkly with static light and nutrient-replete conditions commonly used in laboratory culture experiments. Because field and laboratory growth conditions can be very dissimilar, it is reasonable to expect differences in chl:C_{phyto} photoacclimation patterns between laboratory and field populations. This expectation is illustrated by the photoacclimation response derived from natural phytoplankton communities using satellite observations and that from the laboratory. Specifically, the satellite-based relationship (solid black line in Fig. 1) developed using the 99th percentile of estimated chl:C_{phyto} and monthly median E_g for the surface mixed layer exhibits only a modest decrease of ~2-fold in chl:C_{phyto} from minimum to maximum values of E_g (Behrenfeld et al. 2005, Westberry et al. 2008). Compared to this result, static light nutrient-replete culture experiments show a wider range in chl:C_{phyto} ratio across the same growth irradiances. An extreme example of this is *Dunaliella tertiolecta* which, when grown in constant light, exhibits a nearly 8-fold change in chl:C_{phyto} from minimum to maximum E_g (Behrenfeld et al. 2005, grey dashed line in Fig. 1). Behrenfeld et al. (2002) showed a similarly large range (~6-fold) in chl:C_{phyto} for 21 different phytoplankton species from 23 previously published laboratory studies (see Fig. 1 inset in Behrenfeld et al. 2002). Still, other laboratory studies have reported less dramatic changes, albeit larger than observed in satellite data, in chl:C_{phyto} (~3-fold) over a wide range of growth irradiances (e.g. Laws & Bannister 1980, Geider et al. 1997). An optimality model of resource allocation to light harvesting for cells grown under dynamic and static light conditions was recently described by Talmy et al. (2013). Model results yielded a photoacclimation response curve with a more limited range in light harvesting for a mixed light environment (2.5-fold) than for a static light environment (8-fold) (see Fig. 10 in Talmy et al. 2013). These model results reflect a higher investment of resources into carbon fixation and photoprotection compared to pigment synthesis under mixed light conditions (Talmy et al. 2013), suggesting alternative strategies to pigment synthesis when cells are in a low mean but highly variable light environment. Importantly, the chl:C_{phyto} response from the dynamic light model is very similar to the photoacclimation response derived from satellite data (Fig. 1, solid black and solid grey lines).

Many ecosystem models and satellite algorithms specify relationships between chl:C_{phyto} and E_g to

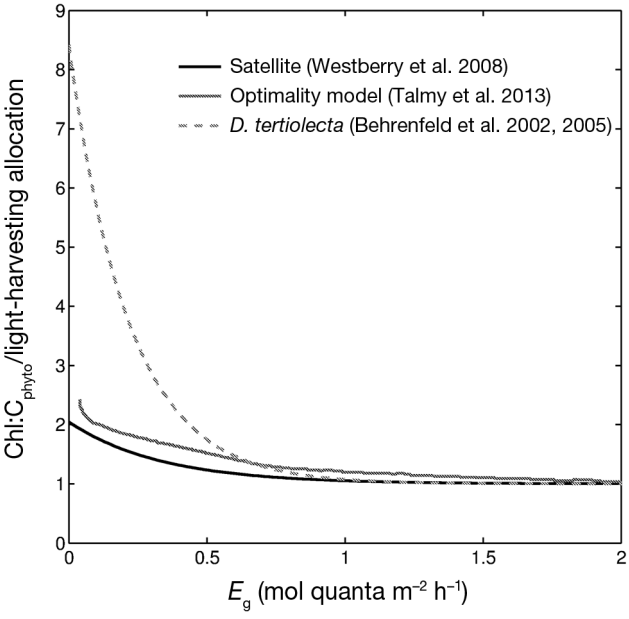

Fig. 1. Photoacclimation relationships (chlorophyll *a*: phytoplankton carbon [chl:C_{phyto}] ratio vs. growth irradiance [E_g]) for satellite retrievals (solid black line), light-harvesting allocation data from an optimality model for cells experiencing fluctuating light (solid grey line from Talmy et al. 2013), and a steady-state nutrient-replete culture of *Dunaliella tertiolecta* (dashed grey line, after Behrenfeld et al. 2005). Data normalized to the minimum chl:C_{phyto} at high light

determine phytoplankton μ and net primary production (NPP) (e.g. Blackford et al. 2004, Westberry et al. 2008). Because relationships describing photoacclimation can differ greatly between field and culture data, parameters from cultures may not be applicable to ecosystem models that do not resolve phytoplankton species, cell size, functional types, etc. More so, the choice of parameters used may differ between studies. For example, the chl:C_{phyto} maxima at low light from Blackford et al. (2004) and the carbon-based production model (CbPM) (Westberry et al. 2008) differ by almost 2-fold (0.075 vs. 0.042, respectively). Such differences may lead to incompatible results between the different models. Furthermore, interpretations of long-term changes in the historical chlorophyll records require an accurate characterization of photoacclimation to discriminate changes due to biomass, light, or nutrients (Behrenfeld et al. 2009, Siegel et al. 2013). And, while different light regimes may result in different photoacclimation responses, as described above, defining a photoacclimation response relationship for natural phytoplankton assemblages in a dynamic light environment is essential for advancing our understanding of ocean ecosystems and the response of microalgal communities to climate forcings.

One of the critical obstacles to evaluating chl:C_{phyto} variability in the field has been the determination of phytoplankton biomass (C_{phyto}). While measurements of chl *a* are routine (Wright et al. 2005), C_{phyto} has traditionally been estimated by proxy or conversion of phytoplankton-related properties (e.g. chlorophyll, cell number or cell volume, total particulate organic carbon). Proxy measurements are subject to large errors and contamination (Banse 1977, Graff et al. 2012). Fortunately, direct measurements of C_{phyto} are now possible by combining sorting flow-cytometry and elemental analysis (Graff et al. 2012, 2015, Casey et al. 2013). These methods can be used to explore phytoplankton biomass distributions in the field (Casey et al. 2013, Graff et al. 2015), constrain global estimates of C_{phyto} from space (Graff et al. 2015), investigate photophysiology, and revise descriptions of phytoplankton physiology and biomass in ecosystem models.

Here, we describe patterns in chl:C_{phyto} observed in the open ocean where both chl *a* and C_{phyto} concentrations were measured analytically. Field samples were collected from a wide range of environmental conditions including the Equatorial Pacific Ocean (EPO) and a north–south transect of the Atlantic Ocean from temperate to oligotrophic waters. Observed chl:C_{phyto} variability is evaluated in the context of mixed-layer light conditions, as well as nutrient concentrations and supply patterns. The primary focus of this report is to compare the new field data with previously described relationships from laboratory- and satellite-based studies, where photoacclimation has been described as a function of average or median light levels (E_g). For the current analysis, we assume that the photoacclimation state of phytoplankton can be described as a function of the median mixed-layer light level (i.e. cells acclimate to the integrated daily mean light level in the mixed layer), but note that this assumption has yet to be rigorously evaluated from the perspective of cellular mechanisms regulating chlorophyll synthesis. We find that the relationship between field-based chl:C_{phyto} data and E_g is more consistent with the satellite-based photoacclimation response than laboratory results which exhibit more extreme responses, e.g. *D. tertiolecta*. To explore the utility of these new results for estimating NPP, we then apply the CbPM (Westberry et al. 2008), which was originally developed for application to satellite data, to the north–south Atlantic Ocean transect data. We compare the resultant production estimates from the CbPM with ^{14}C uptake rates for the Atlantic Meridional Transect (AMT) and assess the estimated growth rates relative to surface nutrient data for which the model employs a relationship between Chl:C_{phyto} ratios and nutrient limited growth rates.

MATERIALS AND METHODS

Field samples from the surface mixed layer and optical measurements were collected during 2 cruises (Fig. 2). The first cruise took place in the EPO from 7 May to 28 June 2012 in conjunction with the National Oceanic and Atmospheric Administration's (NOAA) Tropical Atmospheric Ocean project aboard the NOAA Vessel 'Ka'imimoana' (Fig. 2). The second field effort was part of the 22nd Atlantic Meridional Transect (AMT-22) aboard the RSS 'James Cook' from 10 October to 24 November 2012 (Fig. 2). During both cruises, surface optical properties were continuously measured as described in Dall'Olmo et al. (2009). Discrete samples were collected from the ships' flowing seawater supply for C_{phyto}, high-performance liquid chromatography (HPLC) pigments and total particulate organic carbon (POC) analyses. During the EPO cruise, samples from the surface mixed layer and from depths below the mixed layer were also collected using a CTD rosette with Niskin bottles.

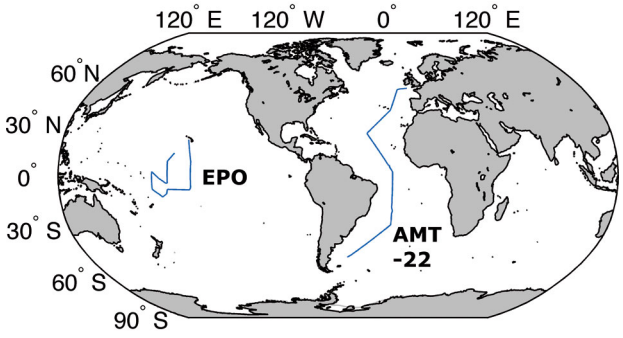

Fig. 2. Ship tracks (blue lines) for 2 cruises used to collect discrete samples and continuous optical measurements: (1) in the Equatorial Pacific Ocean (EPO) (May/June 2012) and (2) the 22nd Atlantic Meridional Transect (AMT-22) (Nov/Dec 2012)

Phytoplankton biomass and pigments

Three methods were used to estimate C_{phyto} in the field: (1) direct analytical measurement (Graff et al. 2012, 2015), (2) biomass particulate backscattering (b_{bp}) at 470 nm (Graff et al. 2015), and (3) cell counts of *Prochlorococcus* converted to carbon. First, direct measurement of C_{phyto} employs sorting flow-cytometry to collect cells for elemental analysis. Details of this procedure can be found in Graff et al. (2015) but are reviewed here briefly. Whole seawater samples were processed on a Becton Dickson Influx Cell Sorter (BD ICS) flow-cytometer and the collected material was analyzed on a Shimadzu TOC-N using manual injection. A sample blank, consisting of artificial seawater (de-ionized water plus sodium chloride) used as sheath fluid in the BD ICS, was analyzed to correct for non-algal carbon contributed by the sheath water to the sorted sample. Second, optically derived C_{phyto} was calculated using measurements of b_{bp} similar to Behrenfeld et al. (2005) and Westberry et al. (2008). However, a newly refined and validated relationship between C_{phyto} and b_{bp} in the field reported in Graff et al. (2015) is used here ($C_{phyto} = 12128 \times b_{bp470} + 0.59$). Last, *Prochlorococcus*-specific carbon was calculated using flow-cytometry determined cell concentrations multiplied by 100 fg C cell^{-1}. Published values of carbon cell^{-1} for *Prochlorococcus* span an order of magnitude from 35 to 350 fg carbon cell^{-1} (Caron et al. 1995 and referenes therein, Veldhuis & Kraay 2004). *Prochlorococcus*-specific carbon was determined because divinyl chl *a* (DV chl) is unique to these cells and can be used to independently evaluate chl:C_{phyto} ratios for this this group. These ratios, however, should be cautiously interpreted given the potential range in carbon for this group.

Whole seawater samples (1–3 l) were filtered onto pre-combusted (450°C, 4 h) glass fiber filters (GF/F) for HPLC pigment analysis. Each filter was immediately placed into a cryovial and stored in liquid nitrogen (LN). Samples were analyzed at the NASA Goddard Space Flight Center Ocean Ecology Laboratory (Van Heukelem & Thomas 2001). Total chl *a* and DV chl are considered here.

Optics and light

Optical parameters were continuously measured on the flow-through seawater systems of both research vessels using a WETLabs ECO-BB3 backscattering sensor (470, 532, and 670 nm) mounted in a custom-made backscattering flow chamber (Dall'Olmo et al. 2009). Particulate backscattering at 470 nm (b_{bp}) was calculated following Dall'Olmo et al. (2009). Values reported here represent up to 60 min averages centered on the time of sample collection for discrete measurements of pigments and/or C_{phyto}. A smaller temporal averaging period was used in temperate waters where increased spatial heterogeneity in particle fields exist.

For the EPO cruise, E_g (mol quanta m^{-2} h^{-1}) was calculated for stations sampled with the CTD rosette using ship-mounted incident photosynthetically active radiation (PAR) measurements and extinction coefficients ($K_d = 0.121 \times chl^{0.428}$) (Morel & Maritorena 2001). E_g values within the mixed layer were calculated as the median light level following Behrenfeld et al. (2005). For the AMT-22 transect, E_g was calculated from the daily noon CTD casts and interpolated to each sample station using the Matlab shape-preserving interpolant, which fits a piecewise polynomial function to the dataset, i.e. fitting a smooth function for E_g between latitudinal data. Mixed-layer depths were determined using the criteria of a change in potential density of 0.125 kg m^{-3} relative to that observed at a depth of 10 m (Levitus 1982).

Modeling NNP

High spatial-resolution estimates of μ, NPP, and nutrient stress were obtained by applying the CbPM (Westberry et al. 2008) to the AMT-22 transect field data. Growth rates and NPP were calculated using the photoacclimation and growth rate parameters developed in Westberry et al. (2008). In the CbPM, the maximum phytoplankton growth rate (μ) is set at 2 divisions (div) d^{-1} as observed in the field (Banse

1991). This maximum is then scaled to account for both light and nutrient limitation of growth rate (Westberry et al. 2008, their Eq. 5). In this approach, the satellite-derived field photoacclimation relationship (Fig. 1, black line) defines the maximum chl:C_{phyto} as a function of E_g where the maximum chl:$C_{phyto} = 0.022 + (0.045 - 0.022)e^{-3PAR(z)}$ (from Westberry et al. 2008, their Eq. 4, z is depth). Where light is saturating for growth, the maximum division rate is 2 and when it is limiting is scaled to a lower value according to the relationship $1 - e^{(-5 \times Eg)}$. A decrease in μ under low light conditions results from a decrease in light absorption as chl synthesis is not sufficient to match the reduction of the light field (Geider 1987, 1996). The exponent −5 describes the strength of light limitation on μ observed in laboratory photoacclimation experiments (Westberry et al. 2008 using M. J. Behrenfeld unpubl. data 2007). This model also incorporates nutrient effects on growth rates. Decreases in chl:C_{phyto} resulting from nutrient limitation are directly proportional to changes in μ (Laws & Bannister 1980, Halsey & Jones 2015). Therefore, an observation of chl:C_{phyto} which is less than the predicted maximum at its determined E_g is attributed to nutrient stress. Fig. 3 is a diagram of this approach for a single observation. In this example, we have an observation (open circle) of chl:C_{phyto} at a particular E_g which falls below the maximum value described by the photoacclimation response curve. The ratio A/B quantifies the reduction in chl:C_{phyto} between the maximum and minimum (μ = 0) growth rates at that E_g due to nutrient limitation. Because it is directly proportional, the ratio of A/B is used to scale μ for nutrient effects. Nutrient stress is calculated from the CbPM as 1 − A/B where a value of zero represents nutrient replete conditions and a value approaching 1 indicates of a high degree of nutrient stress. Thus, we can calculate the division rate of a phytoplankton community for an observed chl:C_{phyto} and E_g and discern which, if any, of these environmental parameters are responsible for limiting growth. Mixed-layer NPP values were calculated as $\mu \times C_{phyto}$ and integrated to the base of the mixed layer. These values are further divided into broad biogeographic regions (after Zubkov et al. 2000) and compared to depth-integrated ^{14}C measurements reported for corresponding provinces for the AMT-22 cruise (Tilstone & Lange 2013) and the historical AMT dataset (Tilstone et al. 2009).

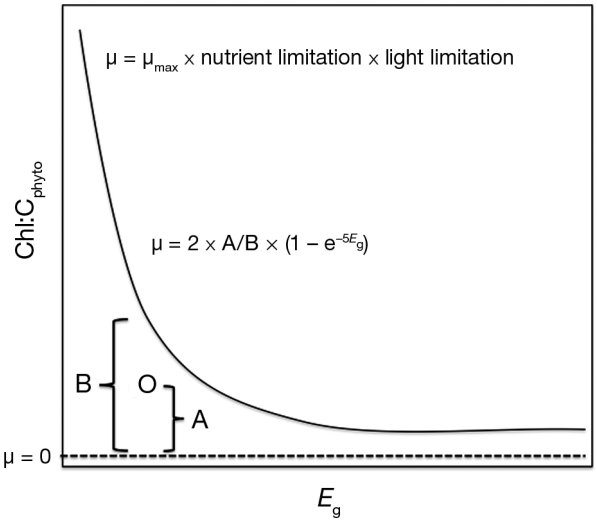

Fig. 3. Diagram of growth rate (μ) calculation used in the carbon-based productivity model (CbPM) (Westberry et al. 2008). Growth rate is scaled from a theoretical maximum of 2 (Banse 1991) by nutrient limitation when observations fall below the solid black line and by light limitation at low light. A: observed chl:C_{phyto}; B: maximum chl:C_{phyto} possible for a given equation; O: observed chl:C_{phyto} and E_g

Nutrient data from the AMT database for samples collected between 2 and 5 m during the 22nd AMT Cruise are included in this study for qualitative analyses of chl:C_{phyto} and CbPM results for μ and nutrient stress terms. Nutrient data for AMT-22 includes inorganic nitrogen (nitrate plus nitrite), phosphate, and silicate.

RESULTS

For the 41 total direct measurements of C_{phyto} presented here, 20 were from discrete samples collected from the EPO and 21 were from the AMT-22 cruise. Biomass directly measured for these samples ranged from 4 to 58 μg l^{-1} (Graff et al. 2015). Applying the b_{bp} vs. C_{phyto} relationship described by Graff et al. (2015) yielded 200 additional indirect estimates of C_{phyto}, and conversions of the *Prochlorococcus* cell counts to biomass added another 159 values specific for that group. Biomass estimates from measurements of b_{bp} along the AMT-22 transect ranged from 6 to 47 μg l^{-1} (Fig. 4B). Chlorophyll was lowest in the southern subtropical region at 0.026 μg l^{-1} and highest in the southern temperate region at 1.13 μg l^{-1} (Fig. 4A). E_g ranged from 0.0022 to 1.9 mol quanta m^{-2} h^{-1} where direct measurements of C_{phyto} were available. Interpolating E_g between CTD stations and to where proxy estimates of biomass were available extended the upper range of growth irradiance for this analysis from 1.9 to 2.8 mol quanta m^{-2} h^{-1} (Fig. 4D).

Chl:C_{phyto} from direct measurements ranged from 0.0023 to 0.032 (Fig. 5A), exhibiting almost 15-fold variability that reflects both nutrient- and light-

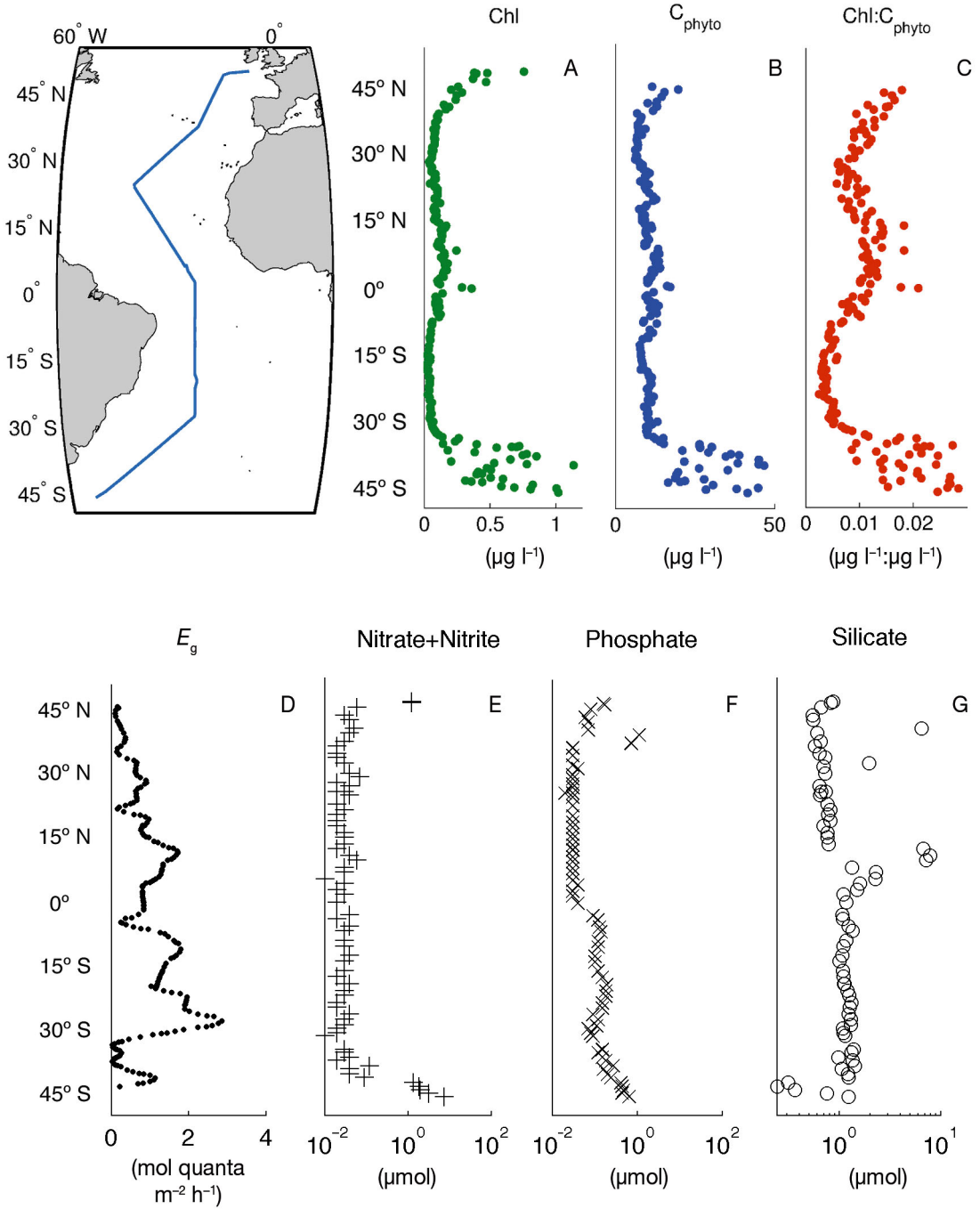

Fig. 4. 22nd Atlantic Meridional Transect (AMT-22) data for (A) high-performance liquid chromatography chlorophyll *a*, (B) biomass particulate backscattering (b_{bp})-estimated phytoplankton carbon (C_{phyto}), (C) chl:C_{phyto}, (D) growth irradiance (E_g), (E) inorganic nitrogen (nitrate plus nitrite), (F) phosphate, and (G) silicate concentrations for samples collected in the upper 10 m during the AMT-22 Cruise

driven changes in cellular pigmentation (Geider 1987, Geider et al. 1997, Behrenfeld et al. 2005). Inclusion of indirect C_{phyto} estimates from b_{bp} or *Prochlorococcus* cell counts significantly increased the number of chl:C_{phyto} observations with collocated estimates of median mixed-layer light level. When biomass was derived using b_{bp} or *Prochlorococcus* cell counts the range of chl:C_{phyto} was 0.003–0.027 (Fig. 5B) and 0.001–0.05 (Fig. 5C), respectively.

Field-derived photoacclimation parameters (chl:C_{phyto} and E_g) were used to model phytoplankton µ and NNP. We calculated phytoplankton division rates fol-

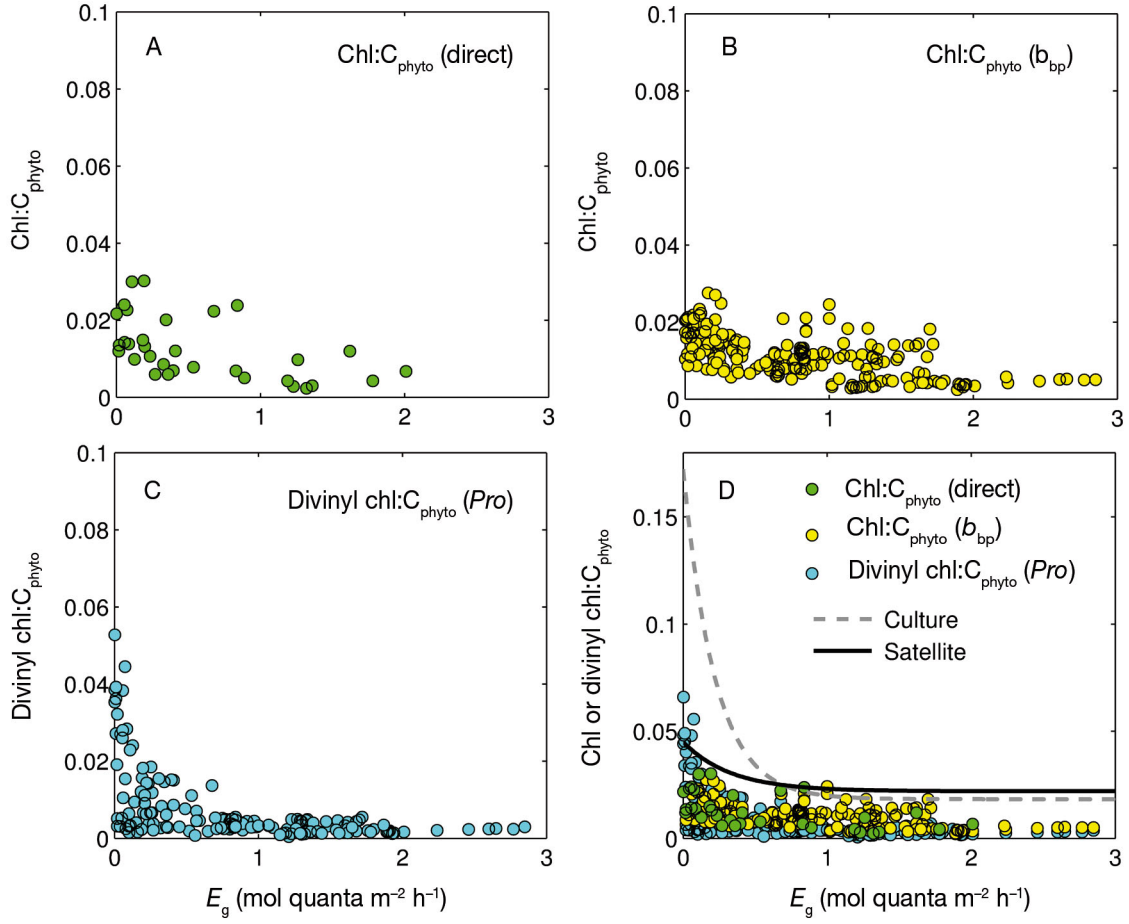

Fig. 5. Chlorophyll *a*: phytoplankton carbon ratio (chl:C_{phyto}) for field samples vs. growth irradiance (E_g) using (A) direct measurements of C_{phyto}, (B) a proxy relationship of biomass particulate backscattering (b_{bp}) (Graff et al. 2015), and (C) divinyl chl:C_{phyto} using carbon from conversions of *Prochlorococcus* (*Pro*) cell concentrations. (D) All data combined. Dashed/solid lines are same as shown in Fig. 1 but are not normalized here as in Fig. 1. Note *y*-axis scale change in (D) to accommodate the continuous light culture data

lowing the approach used in the CbPM (Westberry et al. 2008) and detailed again in this paper. Here, we used C_{phyto} estimates from b_{bp} for the AMT-22 transect to provide high-resolution estimates of μ and NPP. Along the north–south transect, estimates of μ ranged from 0.03 to 1.9 div d^{-1} (Fig. 6B). Division rates were highest at the southern end of AMT-22, and another peak was observed in the vicinity of the Intertropical Convergence Zone (ITCZ) at approximately 12° N. Lower values were observed in the oligotrophic gyres (~0.3 div d^{-1}). NPP in the CbPM is calculated by definition as $\mu \times C_{phyto}$. Mixed-layer NPP from the CbPM approach ranged from 45 to 1447 mg C m^{-2} d^{-1} (Table 1), exhibiting a local peak near the Equator (731 mg C m^{-2} d^{-1}) and the maximum in southern temperate waters (Fig. 6C). Both subtropical gyres had a lower range in NPP, as did the northern temperate region, spanning from 45 to 558 for these 3 regions combined (Table 1).

DISCUSSION

A significant amount of scatter is seen in all chl:C_{phyto} observations (Fig. 5 A–C) and nearly all values fall below the photoacclimation response curves for the *Dunaliella tertiolecta* culture and satellite ocean-color retrievals (Fig. 5D). These response curves (lines in Fig. 5D) represent chl:C_{phyto} under nutrient-replete conditions in culture or optimal growth conditions observed in the field for a particular E_g. Observations that lie below the maximal photoacclimation response curves are attributed in the CbPM to a reduction in chl:C_{phyto} resulting from nutrient-limited growth rate (Laws & Bannister 1980, Halsey & Jones 2015) but may also reflect E_g being an incomplete descriptor of the mixed-layer light level to which phytoplankton photoacclimate. While the field chl:C_{phyto} reported

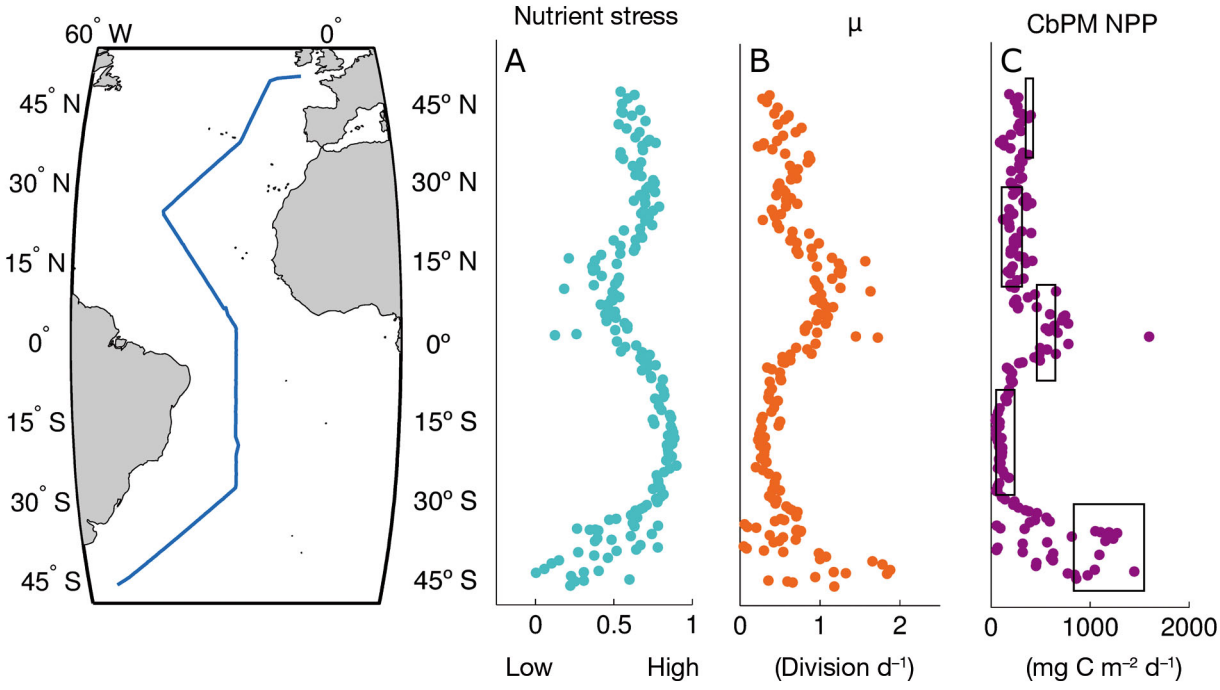

Fig. 6. Application of the carbon-based production model (CbPM) to the 22nd Atlantic Meridional Transect (AMT-22) data (see Fig. 2) provides estimates of (A) nutrient stress, (B) growth rate (μ), and (C) CbPM net primary production (NPP). Regional ranges for AMT-22 ^{14}C–NPP estimates shown by the boxes around CbPM–NPP estimates

Table 1. Comparison of surface mixed-layer net primary production (NPP) using the carbon-based production model (CbPM) (Westberry et al. 2008) with depth-integrated ^{14}C measurements for the same 22nd Atlantic Meridional Transect (AMT-22) cruise and with the historical AMT record (1998–2005)

Region of Atlantic Ocean	Net primary production (mg C m^{-2} d^{-1})		
	CbPM AMT-22	^{14}C AMT-22	^{14}C (1998–2005)
All Regions	45–1447[a]	100–1600	51–1245
Northern temperate (50° N, 40° N)	91–379	~400	51–678
Northern subtropical (40° N, 12° N)	122–417	100–300	137–590
Western tropical Atlantic (12° N, 3° S)	161–779[a]	500–650	51–459
Southern subtropical (3° S, 37° S)	45–558	150–250	89–542
Southern temperate (37° S, 50° S)	57–1447	900–1600	110–1245
Total observations	N = 180	N = 37	N = 91

[a]Excludes 2 observations of 1579 and 2004 mg C m^{-2} d^{-1} at the Equator

here fall below the more extreme laboratory (represented here by *D. tertiolecta*) and satellite-derived photoacclimation responses, the observed maxima closely match those from satellite retrievals (Fig. 5D, solid line). This does not strictly rule out the possibility that the satellite-based photoacclimation relationship or the field observations reported here deviate from the laboratory results due to nutrient limitation. However, the limited range in chl:C_{phyto} from satellite retrievals includes observations in regions where nutrients are seasonally replete. Field data also represent a mixed phytoplankton community that may dampen the photoacclimation response curve relative to culture studies which observe larger changes. For example, the range of chl:C_{phyto} of *Prochlorococcus* (Fig. 5C), not accounting for nutrient impacts on this ratio, appears to be more enhanced relative to the total community (Fig. 5D). Disentangling nutrient, light, and species-specific impacts on the field photoacclimation response curve cannot be fully accomplished here. However, the variability and broad patterns in chl:C_{phyto} along the AMT transect can be explored relative to light and nutrient concentrations.

Chl:C_{phyto} variability along the AMT

In this subsection, we focus on the AMT-22 transect and evaluate the observed patterns in chl:C_{phyto} against *in situ* E_g and nutrient conditions. Enhanced chl:C_{phyto} ratios in the northern temperate region of the transect correspond to low E_g (Fig. 4C,D) and moderately elevated nutrients (Table 2, Fig. 4C & E–G). A more dramatic increase in chl:C_{phyto} is seen in the southern temperate region (Fig. 4) sampled during austral spring. Nitrogen (nitrate + nitrite) and phosphate were maximal in this region (Fig. 4D,E), and E_g was often as low as that encountered in the temperate northern waters (Fig. 4). Thus, low light and increased nutrients underlie the highest chl:C_{phyto} observed during AMT-22. Conversely, the lowest chl:C_{phyto} were found in the North Atlantic Subtropical Gyre (~20–35° N), where nutrients were at a minimum and light was moderately high in comparison to other regions (Table 2, Fig. 4).

Nutrient impacts on chl:C_{phyto} become more apparent when comparing regions of the AMT transect as a function of irradiance (Fig. 7). Chl:C_{phyto} for the southern portion of the transect (Fig. 7, dark blue) fall well above those collected in the northern temperate waters (Fig. 7, dark red) despite having similar E_g values in both regions. A local peak in chl:C_{phyto} was also present just north of the equator at ~15° N in the ITCZ. Nutrient inputs into the ITCZ include upwelling (Robinson et al. 2006) and nitrogen and iron-rich dust blowing off the African continent, which peak in concentration in this region (Baker et al. 2013). Samples from the ITCZ create a cluster of points (Fig. 7, light green, yellow, and light orange) that fall above samples with similar E_g values. Elevated concentrations of silicate are visible in the nutrient data in this region (Table 2, Fig. 4G), and enhanced inputs of iron in the ITCZ would elevate chl:C_{phyto} in this region (Sunda & Huntsman 1997). However, inorganic nitrogen and phosphate do not show increases in the ITCZ. It is likely that one or both of these nutrients are limiting in this region (Moore et al. 2013). Any supply of these nutrients would be quickly taken up and incorporated into biomass and, thus, would not likely be measured as freely available resources.

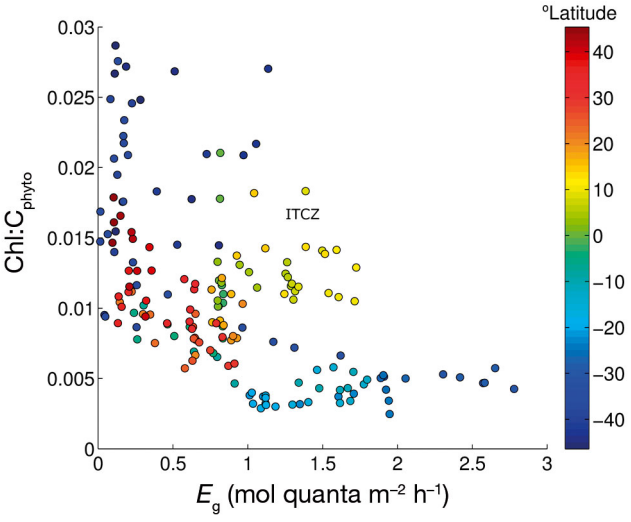

Fig. 7. Chlorophyll *a*: phytoplankton carbon ratio (chl:C_{phyto}) as a function of growth irradiance (E_g) for the 22nd Atlantic Meridional Transect (AMT-22) using the biomass particulate backscattering (b_{bp}) C_{phyto} relationship (b_{bp} vs. C_{phyto}). Samples are color-coded by latitude. Distinct regional groupings can be seen, e.g. elevated chl:C_{phyto} for samples collected in the Intertropical Convergence Zone (ITCZ) (0 to ~17° N) where nitrogen and iron inputs are elevated along this transect

μ and NPP along the AMT

Patterns in chl:C_{phyto} observed for AMT-22 are consistent with our understanding of the environmental parameters which impact these values. Thus, we can evaluate the patterns in μ and NPP derived from the CbPM as it was applied to our field data. In the oligotrophic gyres where μ is low, nutrient stress appears to be relatively high (Fig. 6A). Reduced growth in

Table 2. Range in nutrients, median mixed-layer light (E_g), and the chlorophyll *a*: phytoplankton carbon (chl:C_{phyto}) ratio by region along the 22nd Atlantic Meridional Transect (AMT-22) cruise transect. E_g: growth irradiance

Region of Atlantic Ocean	Nitrate + Nitrite (μmol l^{-1})	Phosphate (μmol l^{-1})	Silicate (μmol l^{-1})	E_g (mol quanta m^{-2} h^{-1})	Chl:C_{phyto} (μg l^{-1}:μg l^{-1})
Northern temperate (50° N, 40° N)	0.04–1.24	0.06–1.1	0.55–6.5	0.09–0.36	0.012–0.017
Northern subtropical (40° N, 12° N)	0.02–0.07	0.02–0.72	0.57–1.96	0.15–1.72	0.006–0.018
Western tropical Atlantic (12° N, 3° S)	0.01–0.06	0.03–0.12	1.06–7.85	0.24–1.34	0.009–0.02
Southern subtropical (3° S, 37° S)	0.01–0.04	0.07–0.19	0.97–1.38	0.24–2.85	0.009–0.027
Southern temperate (37° S, 50° S)	0.04–7.4	0.16–0.64	0.24–1.22	0.02–1.13	0.009–0.028

these regions is the result of nutrient stress, as E_g is generally high and not limiting, especially in the South Atlantic subtropical gyre. Moore et al. (2013) reported that phytoplankton growth and production in as much as 30% of low latitude surface ocean waters is limited by nitrogen supply with the remainder of the ocean limited by iron or other micronutrients. However, light can also limit μ, and this is accounted for in the CbPM. A reduction in μ due to light limitation was observed in the northern temperate waters above 35° N. E_g (Fig. 4D) and μ (Fig. 6B) decline sharply moving northward in this region while nutrient stress (Fig. 6A) remains relatively constant.

A broader understanding of how nutrients differentially influence phytoplankton group-specific growth rates in the field can be ascertained from this data. For example, bulk phytoplankton μ in the ITCZ region ranged from 0.8 to 1.6 d^{-1}. Flow cytometric analysis of samples from this region during AMT-22 showed that the phytoplankton community included *Prochlorococcus*, *Synechococcus*, and eukaryotes (data not shown). Division rates for *Prochlorococcus* from laboratory and field studies range from ~ 0.3 to 1 d^{-1} (Liu et al. 1998, Shalapyonok et al. 1998, Partensky et al. 1999). *Prochlorococcus* division rates appear to be insensitive to increased nutrient supplies relative to other phytoplankton groups (Partensky et al. 1999) and take up nutrients at high rates even in oligotrophic waters (Zubkov et al. 2003). Modeled growth rates of the total phytoplankton community in these regions are above and beyond the published range for *Prochlorococcus* and suggest that the remainder of the community, composed of *Synechococcus* and eukaryotic phytoplankton, have higher rates of division as a result of nutrient supplies in this region.

NPP estimates from the CbPM generally agree with ^{14}C measurements (Table 1, Fig. 6C). Depth-integrated ^{14}C-NPP measurements ranged from 100 to 1600 for AMT-22 and from 51 to 1600 if the historical AMT ^{14}C data is included (Table 1) (Tilstone et al. 2009, Tilstone & Lange 2013). A general pattern of low NPP in the subtropical oligotrophic gyres and higher values at the Equator and in temperate waters is consistent between the 2 methods (Table 1, Fig. 6C). A benefit of implementing the CbPM is that it can provide higher resolution data (N = 180) compared to the ^{14}C method (AMT-22, N = 37, AMT 1998–2005, N = 91) and can capture variability that may otherwise be missed by the spatial resolution of the less frequent incubations. Inclusion of the historical AMT dataset further demonstrates that the CbPM-NPP values fall well within the observed range of ^{14}C data (Table 1).

A variety of factors may contribute to differences in NPP estimates from the CbPM and ^{14}C approach. For example, the CbPM-NPP estimates were calculated for the surface mixed layer only, whereas ^{14}C-NPP was integrated over the euphotic zone. Interpretation of ^{14}C incubation results must also consider incubation time and growth rates of the phytoplankton (Halsey et al. 2013, Pei & Laws 2013). Short-term ^{14}C incubation experiments provide estimates of gross primary production (Halsey et al. 2013). Long-term incubations approach net production (Halsey et al. 2013) but may over or underestimate NPP as a result of phytoplankton species composition (Pei & Laws 2013) and differences in the environmental parameters (e.g. light, temperature) between incubations and *in situ* conditions. Additionally, E_g used here was interpolated between noon CTD cast stations and may not accurately represent the water column where samples were collected. Assumptions of the model, for example maximum division rates of 2 d^{-1} or what defines the growth irradiance, could significantly bias model results. New methods for assessing growth rates in the field may shed light on the maximal growth rates of natural phytoplankton communities (Zubkov 2014) and would directly influence modeled NPP in ecosystems models such as the CbPM. Additional work is needed to resolve discrepancies between modeled and measured rates of NPP, which despite the difference in approach, show good relative agreement.

CONCLUSIONS

A fundamental question that still needs to be addressed is how to appropriately evaluate measured chl:C_{phyto} variability with respect to the ocean's mixed-layer light environment. For consistency with earlier studies, we have chosen to express chl:C_{phyto} data as a function of the median mixed-layer light level. While this assessment of growth irradiance is certainly mathematically convenient, it is not mechanistically based on physiological processes that regulate chlorophyll synthesis in the field, and it does not consider how changes in light over the course of the photoperiod influence these regulatory pathways. Clearly, a major area for future work on photoacclimation in natural systems will be the integration of field measurements of chl:C_{phyto} with mechanistic understandings of cellular photoacclimation and regulation in a fluctuating light environment.

Despite using a simplistic description of mixed-layer growth irradiance, a robust conclusion from the current study is that chl:C_{phyto} variability in the upper open ocean does not exhibit the extreme low-light values observed in static light laboratory experiments. Instead, our analytical field data for natural phytoplankton communities appear more consistent with the rather diminished low-light response earlier derived from field data (Behrenfeld et al. 2002), satellite data (Behrenfeld et al. 2005, Westberry et al. 2008), and the dynamic light model of Talmy et al. (2013). Expanding the field database of measured chl:C_{phyto} values, concurrent with water column measurements of the light field and vertical mixing, will be important for refining our understanding of photophysiology in nature. This understanding is critical for advancing ocean ecosystem modeling, improving assessments of global NNP, and interpreting the satellite record of chlorophyll and carbon variability in response to environmental forcings.

Acknowledgements. This work was funded by NASA Grant NNX10AT70G to M. Behrenfeld. This study was also supported by the UK Natural Environment Research Council National Capability Funding to Plymouth Marine Laboratory and the National Oceanography Centre, Southampton. This is contribution number 261 of the AMT Programme. We thank the NOAA Tropical Atmospheric Ocean Program and LCDR Brian Lake and the 22nd Atlantic Meridional Transect Programme and the Principal Scientist Glen Tarran for providing field support to carry out this research.

LITERATURE CITED

Alderkamp AC, Mills MM, van Dijken GL, Arrigo KR (2013) Photoacclimation and non-photochemical quenching under *in situ* irradiance in natural phytoplankton assemblages from the Amundsen Sea, Antarctica. Mar Ecol Prog Ser 475:15–34

Backhaus JO, Wehde H, Hegseth EN, Kämpf J (1999) 'Phyto-convection': the role of oceanic convection in primary production. Mar Ecol Prog Ser 189:77–92

Baker AR, Adams C, Bell TG, Jickells TD, Ganzeveld L (2013) Estimation of atmospheric nutrient inputs to the Atlantic Ocean from 50°N to 50°S based on large-scale field sampling: iron and other dust-associated elements. Global Biogeochem Cycles 27:755–767

Banse K (1977) Determining the carbon-to-chlorophyll ratio of natural phytoplankton. Mar Biol 41:199–212

Banse K (1991) Rates of phytoplankton cell division in the field and in iron enrichment experiments. Limnol Oceanogr 36:1886–1898

Behrenfeld MJ, Marañón E, Siegel DA, Hooker SB (2002) Photoacclimation and nutrient-based model of light-saturated photosynthesis for quantifying oceanic primary production. Mar Ecol Prog Ser 228:103–117

Behrenfeld MJ, Boss E, Siegel DA, Shea DM (2005) Carbon-based ocean productivity and phytoplankton physiology from space. Global Biogeochem Cycles 19, GB1006, doi: 10.1029/2004GB002299

Behrenfeld MJ, Westberry TK, Boss ES, O'Malley RT and others (2009) Satellite-detected fluorescence reveals global physiology of ocean phytoplankton. Biogeosciences 6:779–794

Blackford JC, Allen JI, Gilbert FJ (2004) Ecosystem dynamics at six contrasting sites: a generic modelling study. J Mar Syst 52:191–215

Caron DA, Dam HG, Kremer P, Lessard EJ and others (1995) The contribution of microorganisms to particulate carbon and nitrogen in surface waters of the Sargasso Sea near Bermuda. Deep-Sea Res 42:943–972

Casey JR, Aucan JP, Goldberg SR, Lomas MW (2013) Changes in partitioning of carbon amongst photosynthetic pico-and nano-plankton groups in the Sargasso Sea in response to changes in the North Atlantic Oscillation. Deep-Sea Res II 93:58–70

Cloern J, Grenz C, Vidergar-Lucas L (1995) An empirical model of the phytoplankton chlorophyll: carbon ratio the conversion factor between productivity and growth rate. Limnol Oceanogr 40:1313–1321

Cullen JJ, Lewis MR (1988) The kinetics of algal photoadaptation in the context of vertical mixing. J Plankton Res 10: 1039–1063

D'Asaro EA (2008) Convection and the seeding of the North Atlantic bloom. J Mar Syst 69:233–237

Dall'Olmo G, Westberry TK, Behrenfeld MJ, Boss E, Slade WH (2009) Significant contribution of large particles to optical backscattering in the open ocean. Biogeosci 6: 947–967

Denman K, Gargett A (1983) Time and space scales of vertical mixing and advection of phytoplankton in the upper ocean. Oceanography 28:801–815

Falkowski PG, LaRoche J (1991) Acclimation to spectral irradiance in algae. J Phycol 27:8–14

Geider RJ (1987) Light and temperature dependence of the carbon to chlorophyll *a* ratio in microalgae and cyanobacteria: implications for physiology and growth of phytoplankton. New Phytol 106:1–34

Geider RJ, MacIntyre HL, Kana TM (1996) A dynamic model of photoadaptation in phytoplankton. Limnol Oceanogr 41:1–15

Geider RJ, MacIntyre HL, Kana TM (1997) Dynamic model of phytoplankton growth and acclimation: responses of the balanced growth rate and the chlorophyll *a*:carbon ratio to light, nutrient-limitation and temperature. Mar Ecol Prog Ser 148:187–200

Graff JR, Milligan AJ, Behrenfeld MJ (2012) The measurement of phytoplankton biomass using flow-cytometric sorting and elemental analysis of carbon. Limnol Oceanogr Methods 10:910–920

Graff JR, Westberry TK, Milligan AJ, Brown MB and others (2015) Analytical phytoplankton carbon measurements spanning diverse ecosystems. Deep-Sea Res I 102:16–25

Halsey KH, Jones BM (2015) Phytoplankton strategies for photosynthetic energy allocation. Annu Rev Mar Sci 7: 265–297

Halsey KH, O'Malley RT, Graff JR, Milligan AJ, Behrenfeld MJ (2013) A common partitioning strategy for photosynthetic products in evolutionarily distinct phytoplankton species. New Phytol 198:1030–1038

Havelková-Doušová H, Prášil O, Behrenfeld MJ (2004) Photoacclimation of *Dunaliella tertiolecta* (Chlorophyceae) under fluctuating irradiance. Photosynthetica 42:273–281

Laws EA, Bannister T (1980) Nutrient- and light-limited growth of *Thalassiosira fluviatilis* in continuous culture,

with implications for phytoplankton growth in the ocean. Limnol Oceanogr 25:457–473

Levitus S (1982) Climatological atlas of the world ocean. NOAA Professional Paper 13, US Government Printing Office, Washington, DC

Lewis MR, Cullen JJ, Platt T (1984) Relationships between vertical mixing and photoadaptation of phytoplankton: similarity criteria. Mar Ecol Prog Ser 15:141–149

Liu H, Campbell L, Landry MR, Nolla HA, Brown SL, Constantinou J (1998) *Prochlorococcus* and *Synechococcus* growth rates and contributions to production in the Arabian Sea during the 1995 southwest and northeast monsoons. Deep-Sea Res II 45:2327–2352

MacIntyre HL, Kana TM, Anning T, Geider RJ (2002) Photoacclimaion of photosynthesis irradiance response curves and photosynthetic pigments in microalgae and cyanobacteria. J Phycol 38:17–38

Milligan AJ, Aparicio UA, Behrenfeld MJ (2012) Fluorescence and nonphotochemical quenching responses to simulated vertical mixing in the marine diatom *Thalassiosira weissflogii.* Mar Ecol Prog Ser 448:67–78

Miloslavina Y, Grouneva I, Lambrev PH, Lepetit B, Goss R, Wilhelm C, Holzwarth AR (2009) Ultrafast fluorescence study on the location and mechanism of non-photochemical quenching in diatoms. Biochim Biophys Acta 1787: 1189–1197

Moore CM, Mills MM, Arrigo KR, Berman-Frank I and others (2013) Processes and patterns of oceanic nutrient limitation. Nat Geosci 6:701–710

Morel A, Maritorena S (2001) Bio-optical properties of oceanic waters: a reappraisal. J Geophys Res Oceans 106:7163–7180

Partensky F, Blanchot J, Vaulot D (1999) Differential distribution and ecology of *Prochlorococcus* and *Synechococcus* in oceanic waters: a review. In: Charpy L, Larkum AWD (eds) Marine cyanobacteria. No. spécial 19. Bulletin de l'Institut oceanographique, Monaco, p 457–475

Pei S, Laws EA (2013) Does the ^{14}C method estimate net photosynthesis? Implications from batch and continuous culture studies of marine phytoplankton. Deep-Sea Res I 82:1–9

Robinson C, Poulton AJ, Holligan PM, Baker AR and others (2006) The Atlantic Meridional Transect (AMT) Programme: a contextual view 1995–2005. Deep-Sea Res II 53:1485–1515

Schubert H, Sagert S, Forster RM (2001) Evaluation of the different levels of variability in the underwater light field of a shallow estuary. Helgol Mar Res 55:12–22

Shalapyonok A, Olson RJ, Shalapyonok LS (1998) Ultradian growth in *Prochlorococcus* spp. Appl Environ Microbiol 64:1066–1069

Siegel DA, Behrenfeld MJ, Maritorena S, McClain C and others (2013) Regional to global assessments of phytoplankton dynamics from the SeaWiFS mission. Remote Sens Environ 135:77–91

Sunda WG, Huntsman SA (1997) Interrelated influence of iron, light and cell size on marine phytoplankton growth. Nature 390:389–392

Talmy D, Blackford J, Hardman-Mountford NJ, Dumbrell AJ, Geider RJ (2013) An optimality model of photoadaptation in contrasting aquatic light regimes. Limnol Oceanogr 58:1802–1818

Tilstone G, Lange P (2013) Phytoplankton photosynthesis, primary production and coloured dissolved organic material. In: Tarran G (Principal Scientist) AMT22 Cruise Report, Plymouth Marine Laboratory, Plymouth, p 43–47

Tilstone G, Smyth T, Poulton A, Hutson R (2009) Measured and remotely sensed estimates of primary production in the Atlantic Ocean from 1998 to 2005. Deep-Sea Res II 56:918–930

van de Poll WH, Buma AGJ, Visser RJW, Janknegt PJ, Villafane VE, Helbling EW (2010) Xanthophyll cycle activity and photosynthesis of *Dunaliella tertiolecta* (Chlorophyceae) and *Thalassiosira weissflogii* (Bacillariophyceae) during fluctuating solar radiation. Phycologia 49:249–259

Van Heukelem L, Thomas CS (2001) Computer-assisted high-performance liquid chromatography method development with applications to the isolation and analysis of phytoplankton pigments. J Chromatogr A 910:31–49

Veldhuis MJW, Kraay GW (2004) Phytoplankton in the subtropic Atlantic Ocean: towards a better assessment of biomass and composition. Deep-Sea Res I 51:507–530

Westberry T, Behrenfeld MJ, Siegel DA, Boss E (2008) Carbon-based primary productivity modeling with vertically resolved photoacclimation. Global Biogeochem Cycles 22, GB2024, doi:10.1029/2007GB003078

Wright S, Jeffrey S, Mantoura R (2005) Phytoplankton pigments in oceanography: guidelines to modern methods. Unesco Publishing, Paris

Zubkov MV (2014) Faster growth of the major prokaryotic versus eukaryotic CO_2 fixers in the oligotrophic ocean. Nat Commun 5:3776, doi:10.1038/ncomms4776

Zubkov MV, Sleigh MA, Burkill PH, Leakey RJG (2000) Picoplankton community structure on the Atlantic Meridional Transect: a comparison between seasons. Prog Oceanogr 45:369–386

Zubkov MV, Fuchs BM, Tarran GA, Burkill PH, Amann R (2003) High rate of uptake of organic nitrogen compounds by *Prochlorococcus* cyanobacteria as a key to their dominance in oligotrophic oceanic waters. Appl Environ Microbiol 69:1299–1304

Editorial responsibility: Steven Lohrenz, New Bedford, Massachusetts, USA

Submitted: February 5, 2015; Accepted: November 1, 2015
Proofs received from author(s): January 8, 2016